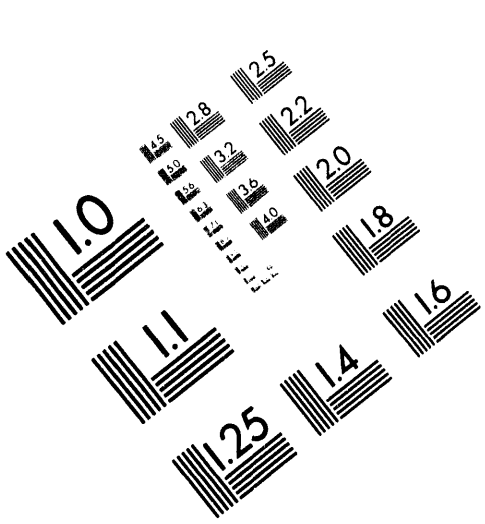

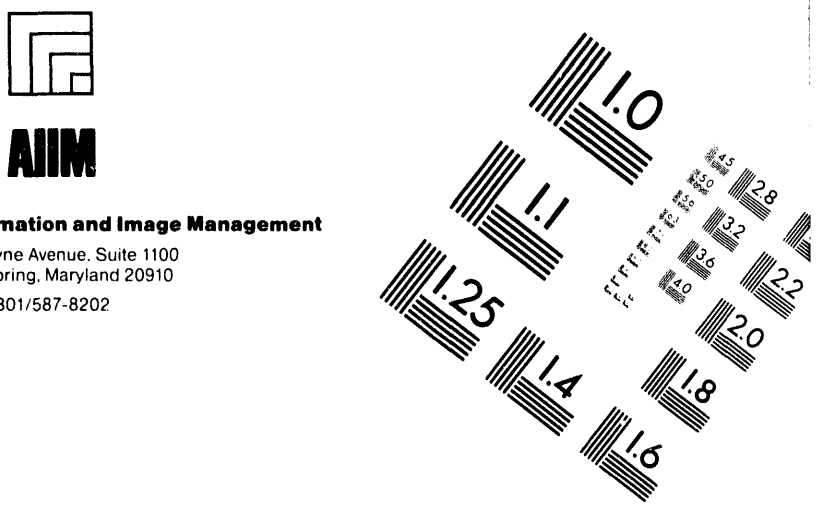

Association for Information and Image Management
1100 Wayne Avenue, Suite 1100
Silver Spring, Maryland 20910
301/587-8202

Centimeter

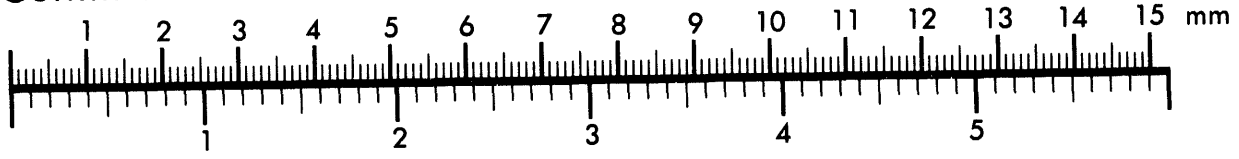

Inches

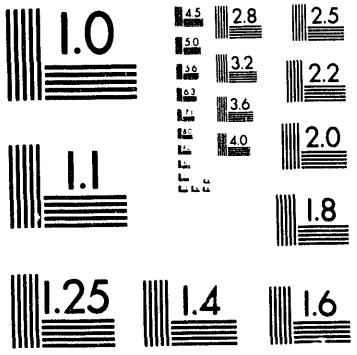

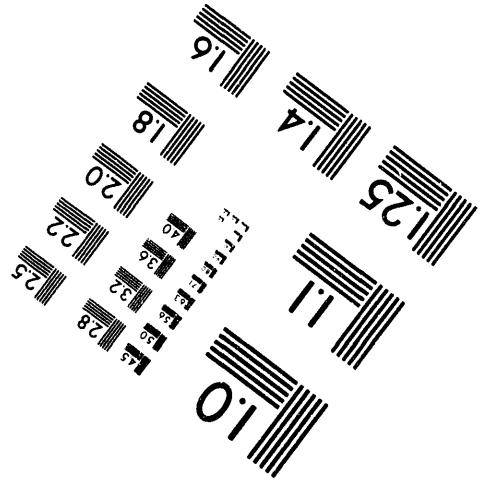

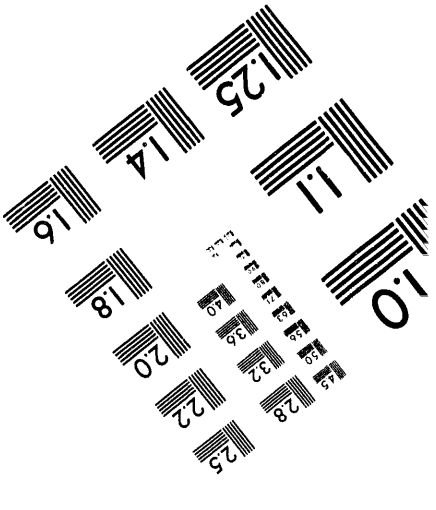

MANUFACTURED TO AIIM STANDARDS
BY APPLIED IMAGE, INC.

1 of 1

2

Conf-930803--32

An Overview of the HSST Full-Thickness Shallow-Crack Clad Beam Testing Program*

J. A. Keeney, T. J. Theiss, W. J. McAfee, B. R. Bass
Oak Ridge National Laboratory, Oak Ridge, TN USA

DISCLAIMER

ABSTRACT

A testing program is described that will utilize full-thickness clad beam specimens to quantify fracture toughness for shallow flaws in material for which metallurgical conditions are prototypic of those found in reactor pressure vessels (RPVs). The beam specimens are fabricated from a section of an RPV wall that includes weld, plate and clad material. Metallurgical factors potentially influencing fracture toughness for shallow flaws in the beam specimen include material gradients due to welding and cladding applications, as well as material inhomogeneities in welded regions due to reheating in multiple weld passes. Fracture toughness tests focusing on shallow flaws in plate and weld material will also provide data for evaluating the relative influence of absolute and normalized crack depth on constraint conditions. Pretest finite-element analyses are described that provide near-tip stress and strain fields for characterization of constraint in the shallow-crack specimens in terms of the Q-stress. Analysis results predict a constraint loss in the shallow-crack clad beam specimen similar to that determined for a previously tested shallow-crack single-edge notch homogeneous bend specimen with the same normalized crack depth.

1 INTRODUCTION

The limiting conditions for reactor pressure vessel (RPV) life assessments frequently are postulated pressurized-thermal-shock (PTS) accident conditions. Analyses of PTS conditions are based on the Marshall flaw distribution (Marshall et al. 1982), Reg. Guide 1.154 (U. S. Nuclear Regulatory Commission), and data from deep-crack fracture toughness specimens. The Marshall flaw distribution predicts more small than large flaws, while Reg. Guide 1.154 requires that all flaws be considered as surface flaws. Probabilistic fracture-mechanics analyses of an RPV have shown that shallow cracks dominate the conditional probability of vessel failure in a PTS evaluation (Cheverton et al. 1985). Therefore, the shallow surface crack is of major importance in RPV life assessments.

A shallow-crack fracture-toughness testing program (Theiss et al. 1992) has shown that shallow-crack specimens (cut from homogeneous plate material) exhibit a toughness significantly higher than conventional deep-crack specimens in the transition temperature region. The apparent toughness increase for shallow flaws is due to a loss of constraint at the crack tip because of the close proximity of the crack-tip plastic zone to the nearest free surface. The shallow-crack program has tested A 533 Grade B (A 533 B) Class 1 steel single-edge notch bend (SENB) specimens with an approximate 100 mm beam depth and beam thicknesses of 51, 102,

*Research sponsored by the Office of Nuclear Regulatory Research, U.S. Nuclear Regulatory Commission under Interagency Agreement 1886-8011-9B with the U.S. Department of Energy under Contract DE-AC05-84OR21400 with Martin Marietta Energy Systems, Inc.

and 152 mm. Beams with a crack depth of ~10 mm (a/W = 0.1) are characterized by a toughness curve shifted -35°C from the deep-crack toughness curve. The specimen depth and crack depth selected for these clad beam tests allow for interpretation of the data in terms of absolute crack depth (a) or normalized crack depth (a/W), both of which have been used in previous investigations to define the shallow-crack effect.

In addition to this shallow-flaw effect, other differences in material conditions exist between conventional deep-crack laboratory specimens and RPVs that could significantly affect fracture toughness. First, shallow flaws in an RPV are located in the near-surface region of clad plate or weld material where metallurgical gradients or inhomogeneities exist. Irwin and Zhang (1992) performed material gradient studies on a large weld section joining two forged A 508 shells of a cladded RPV. They found hardness elevations in the A 508 material due to the reheat cycle of the cladding process that were comparable to those in the heat-affected-zones adjacent to the weld. Irwin and Zhang indicate that these hardness elevations probably translate into a reduction of cleavage initiation toughness. Second, fracture toughness curves used in RPV assessments are based on data from deep-crack L-T oriented fracture toughness specimens taken from the center, homogeneous region of source plates. Axial cracks in plate material of an RPV are oriented in the L-S material direction rather than the L-T orientation. Third, reheating due to multiple passes in the welding process leads to inhomogeneities of microstructure and hardness within the weld metal (Irwin et al. 1992). Finally, any residual stresses that remain after the usual post-weld stress relief heat treatment cycle could affect fracture behavior.

This paper describes a testing program designed to investigate some of the effects of these different conditions on fracture toughness. Several full-thickness clad beam specimens taken from the RPV of a canceled nuclear plant will be tested to investigate the influence of metallurgical gradients, weld inhomogeneities and the cladding process on the fracture toughness of material containing shallow flaws. Specifically, fracture toughness data will be generated from three-point bend specimens (229 x 226 mm cross section) fabricated from full-thickness RPV clad, weld and plate material. Shallow flaws in these beams will be located in material in which metallurgical conditions are prototypic of those found in RPVs. Comparison of results from these tests with those from homogeneous shallow-flaw test specimens will quantify effects of some near surface conditions on fracture toughness. In addition, clad beam fracture toughness tests conducted in plate material can be compared with the homogeneous shallow-crack test results to provide data concerning the relative influence of absolute and normalized crack depth on constraint. The effective fracture toughness from these large beams will also be compared with the toughness as determined by current American Society of Mechanical Engineers (ASME) Section XI rules (The ASME Boiler and Pressure Vessel Code 1989). A review of the test matrix, toughness estimation techniques, and pretest analysis results for the first three tests will be discussed in the following sections.

2 TEST SPECIMEN

2.1 Specimen Preparation and Material Properties

The specimens (see Fig. 1) will be single edge-notch arc beams 229 mm thick, 226 mm deep (W), with an effective span of 1219 mm. The source plate of the specimens consists of welded sections of A 533 B steel with an overlay of stainless steel cladding. All specimens will be notched on the clad surface with flaw depths ranging from 10 to 114 mm. Initial specimens will have the flaw located in an axial weld, while future specimens will have the flaw located in base material. The notch will be a through-thickness, two-dimensional (2-D) flaw penetrating the cladding. The material properties (see Table 1) and stress-strains curves* were provided by the Oak Ridge National Laboratory.

Table 1. Material properties

	Base metal	Weld metal	Cladding
Modulus of elasticity (E), MPa	200,000	200,000	152,000
Poisson's ratio (ν)	0.3	0.3	0.3
Yield stress (σ_0), MPa	440	487	367

*Personal communication to T. J. Theiss, ORNL, from F. M. Haggag, ORNL, July 24, 1992.

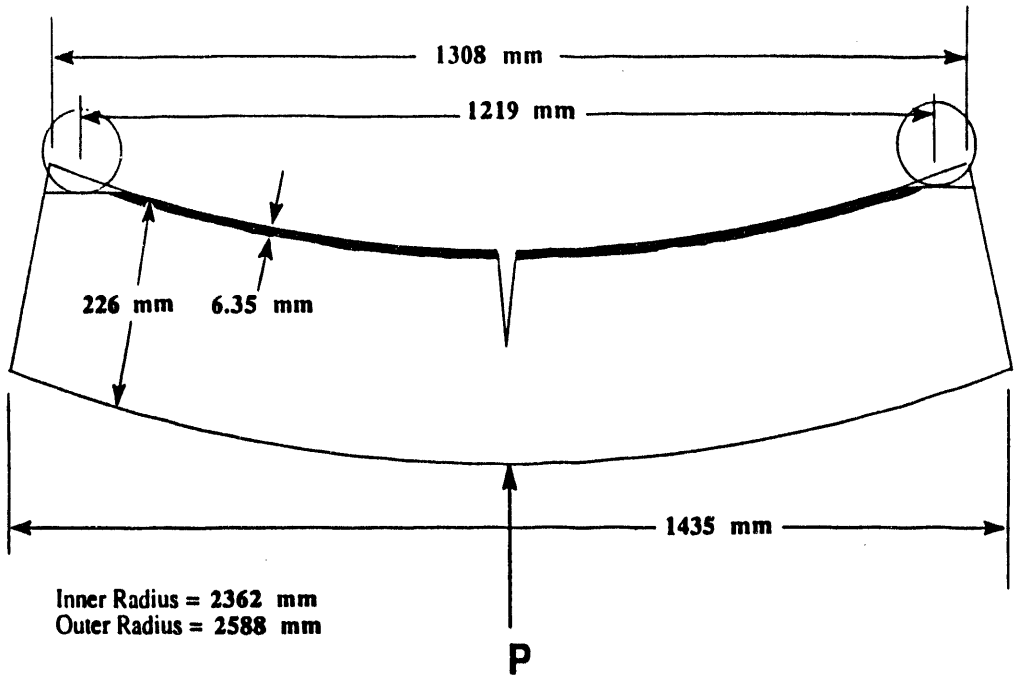

Fig. 1. ORNL clad beam design.

2.2 Test Matrix

Three beams will be tested in the first series, each with the flaw located in axial weld material. The first beam will be used to verify and validate testing procedures. The proposed crack depths, a, shown in Table 2 for the three specimens are after fatigue precracking. The results will be compared with the HSST shallow-crack data for an absolute crack depth of 10 mm and a/W of 0.1. The tentative test temperature for all three beams has been set at $T - RT_{NDT} = -20°C$.

Table 2. Test matrix for clad beam tests

Test beam #	Crack depth, a (mm)	a/W
1	114	0.500
2	23	0.100
3	10	0.045

3 CLAD BEAM PRETEST ANALYSES

Pretest analysis of the three clad beam specimens was conducted to aid in instrumentation selection, to compare with experimental results, and to quantify the expected constraint loss in the shallow-crack geometries. The Q-stress parameter (O'Dowd et al. 1991) is used to correlate constraint losses. Posttest analyses of the shallow- and deep-crack SENB specimens (Theiss et al. 1992) also used the Q-stress parameter to quantify constraint loss. Those analyses indicated a Q-stress at initiation of ~ –0.65 for the shallow-crack specimens and Q ~ 0 for the deep-crack specimens. These analysis results are consistent with the experimental data which produced shallow-crack toughness values ~3.5 times the deep-crack toughnesses in terms of the J-integral. The SENB specimens were taken from the homogeneous center portion of a plate while the initial clad beam tests will sample axial weld material. As a consequence, the pretest analysis for the clad beam specimens will not be able to "predict" fracture toughness, but rather provide an analytical basis for comparison of the deep- and shallow-crack toughness results in the clad beam specimens.

3.1 Analysis Methods

A 2-D finite-element model of the three-point bend specimen, shown in Fig. 2, incorporates the curvature of the plate (inner radius of 2362 mm and outer radius of 2588 mm) and the cut-out to support the specimen end during loading. From symmetry conditions, only half of the specimen

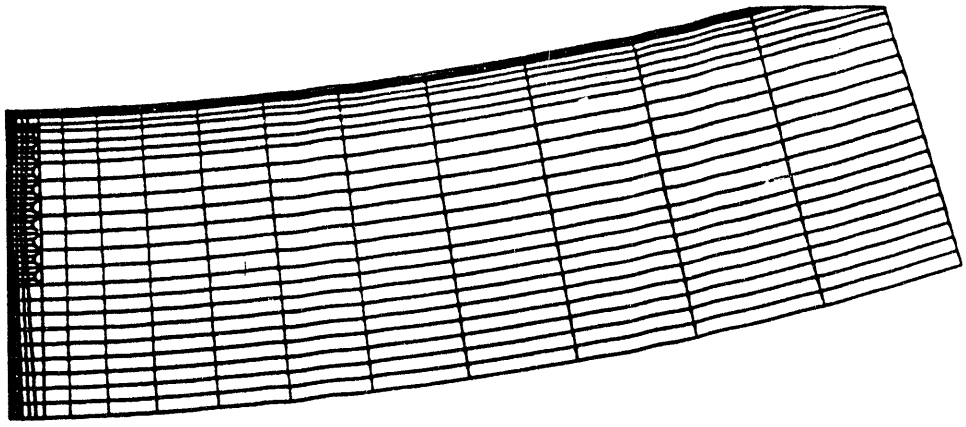

Fig. 2. 2-D finite-element model of the clad beam.

is included in the finite-element model. A separate model was generated for each crack depth in Table 2. Plane-strain analyses, for loads up to approximately 80 to 90% of the limit load (P_L) of each specimen, were performed with the ADINA (Bathe 1978) finite-element code using an incremental elastic-plastic constitutive model and small-strain theory. Any residual stress effects were ignored in these analyses. Various parameters evaluated in these analyses include stress-intensity factor, J-integral, crack-tip opening displacement, crack-mouth opening displacement, load-line displacement, and surface strains along the crack plane. The Q-stresses (O'Dowd et al. 1991) were calculated from near-tip opening-mode stress fields. Some pretest assessments of the clad-beam specimen were made based on these parameters.

3.2 Analysis Results

An initial objective of the pretest clad-beam analyses was to evaluate the loss of constraint in the shallow-crack geometry and compare the results with SENB shallow-crack specimens tested previously (Theiss et al. 1992). The Q-stress parameter is defined as the difference between the "opening-mode" stress component obtained from small-strain, plane-strain, finite-element analyses of the shallow-crack clad beam specimens and the corresponding stress component from the small-scale yielding (SSY) reference solution at a set distance ahead of the crack tip. In these analyses, the deep-crack specimen results at a low load (40% of P_L) are used as an approximation to the SSY reference solution. Earlier analyses (Theiss et al. 1992) have shown that the Q-stress is approximately zero for the deep-crack specimens under these loading conditions.

Distributions of the "opening-mode" stress component (σ_y) for the three specimens are illustrated in Fig. 3. The stress component is normalized by the initial yield stress (σ_0) of the weld material (location of the flaw). Distance ahead of the blunting notch tip is expressed in terms of the normalized distance parameter $r/(J/\sigma_0)$, where r is distance ahead of the crack tip and J is the value of the J-integral associated with the specified loading conditions. Two load cases are plotted for each shallow-crack specimen (the load which produced a J value comparable to the critical J value in the SENB shallow-crack tests described by Theiss et al. (1992), and the maximum load in the present analysis). Results in Fig. 3 indicate that the crack-tip fields in both shallow-crack clad beam specimens deviate significantly from the reference crack-tip solution ($a/W \sim 0.5$, $P = 40\%\ P_L$) as the load levels increase. In other words, the analysis results indicate that the shallow-crack specimens will exhibit a substantial loss of constraint compared with the deep-crack specimen.

In Fig. 4, the J-Q trajectories for the shallow-crack clad-beam specimens are compared with the shallow-crack SENB specimen ($a = 10$ mm, $a/W = 0.1$) tested previously by Theiss et al. (1992). The Q-stress is evaluated at $r/(J/\sigma_0) = 2$ for consistency with the shallow-flaw homogeneous beam analyses (Theiss et al. 1992). Results from the pretest analyses of the clad beam specimens are consistent with the posttest analysis of the SENB specimens. As expected, the analysis also indicates a greater constraint loss for the shallower crack in the clad beam geometry. Initially, the J-Q trajectory of the SENB shallow-crack specimen is bounded by the two shallow-crack clad beam J-Q trajectories; however, the J-Q trajectory in the SENB specimen intersects the trajectory of the clad beam with the same normalized crack depth. Thus, based on J-Q methodology, a

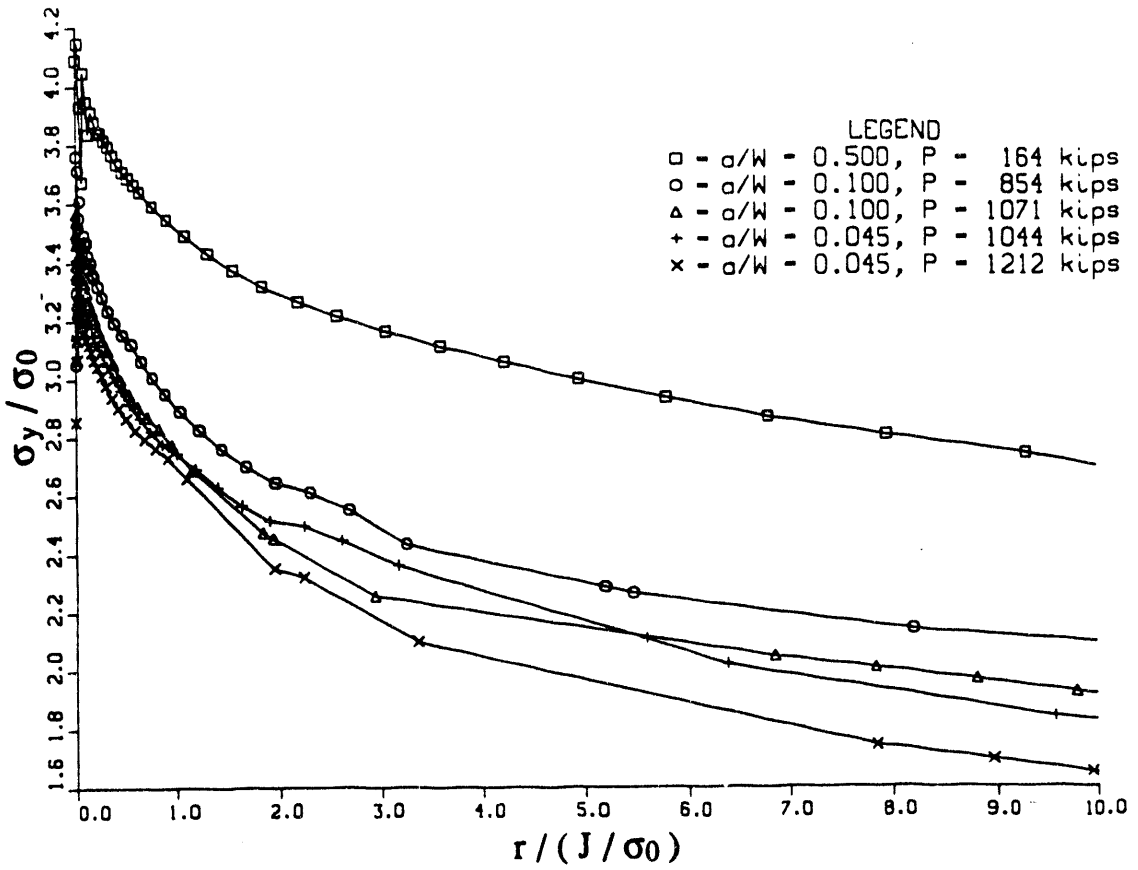

Fig. 3. Distributions of opening-mode stress component for the clad beam specimens.

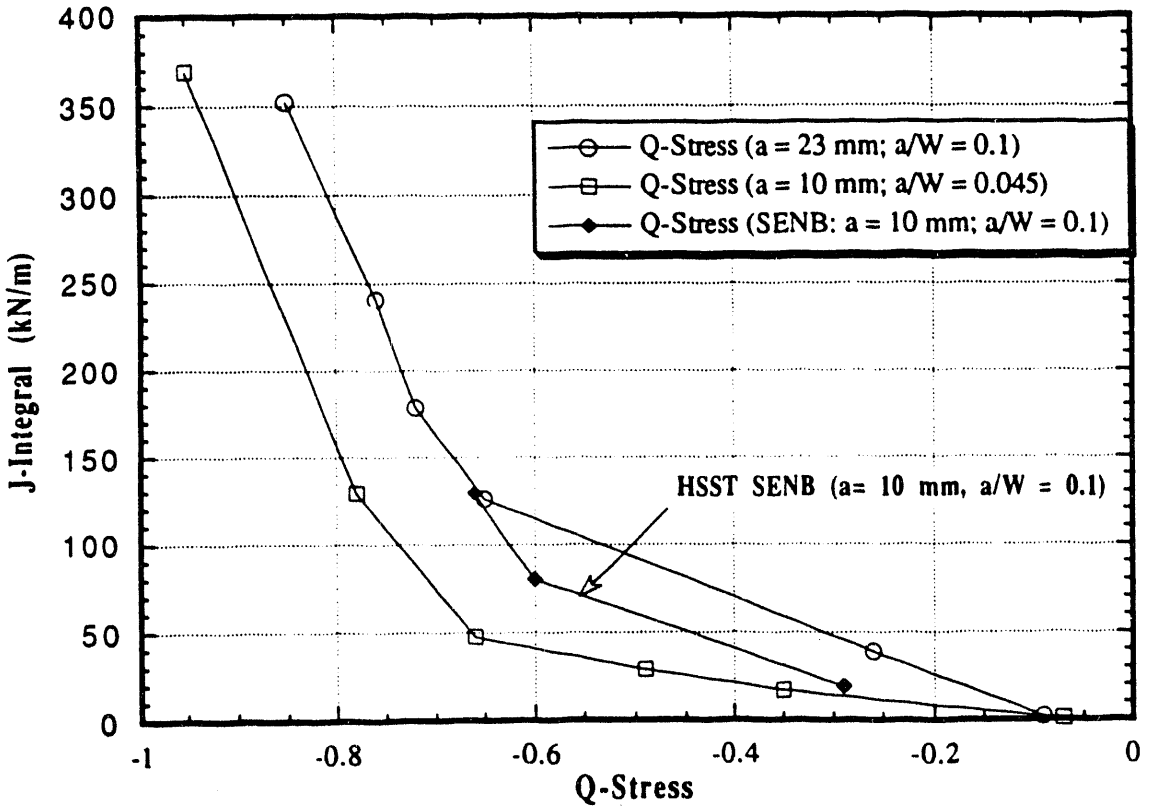

Fig. 4. J-Q trajectories for the shallow-crack beam specimens.

constraint loss and toughness elevation in the shallow-crack clad beam specimen (a/W = 0.1) is expected to be similar to that experienced in the SENB shallow-crack homogeneous specimens with equivalent a/W ratios.

4 SUMMARY AND DISCUSSION

Full-thickness clad beams will be tested to quantify fracture toughness for shallow flaws located in material for which metallurgical conditions are prototypic of those found in RPVs. Pretest finite element analyses have been performed to obtain near-tip stress and strain fields. The opening-mode stress component was used to evaluate the Q-stress parameter for the shallow-crack specimens. The results predict a constraint loss in the shallow-crack clad beam specimen (a/W = 0.1) similar to that measured in the shallow-crack SENB homogeneous specimen with a crack depth a = 10 mm and the same normalized crack depth.

REFERENCES

Bathe, K. J. (1978). *ADINA—A Finite-Element Program for Automatic Dynamic Incremental Non-Linear Analysis*, Report 82448-1, Massachusetts Institute of Technology.

Cheverton, R. D. and Ball, D. G. (1985). Martin Marietta Energy Systems, Inc., Oak Ridge Natl. Lab., *Pressurized-Thermal-Shock Evaluation of the Calvert Cliffs Nuclear Power Plant*, pp. 201–244, NUREG/CR-4022 (ORNL/TM-9408).

Irwin, G. R. and Zhang, X. J. (1985). Martin Marietta Energy Systems, Inc., Oak Ridge Natl. Lab., *Gradient Study of a Large Weld Joining Two Forged A 508 Shells of the Midland Reactor Vessel*, NUREG/CR-5867 (ORNL/Sub/79-7778/10).

O'Dowd, N. P., and Shih, C. F. (1991). *Family of Crack-Tip Fields Characterized by a Triaxiality Parameter: Part I—Structure of Fields*, Journal of the Mechanics and Physics of Solids, Vol. 39, pp. 989–1015.

Marshall, W., et al. (1982). *An Assessment of the Integrity of PWR Pressure Vessels*, UKAEA Study Group Reports.

The American Society of Mechanical Engineers Boiler and Pressure Vessel Code (1989). Section XI, "Rules for Inservice Inspection of Nuclear Power Plant Components."

Theiss, T. J., Shum D. K., and Rolfe, S. T. (1992). Martin Marietta Energy Systems, Inc., Oak Ridge Natl. Lab., *Experimental and Analytical Investigation of the Shallow-Flaw Effect in Reactor Pressure Vessels*, NUREG/CR-5886 (ORNL/TM-12115).

U. S. Nuclear Regulatory Commission (1987). *Regulatory Guide 1.154*, "Format and Content of Plant-Specific Pressurized Thermal Shock Safety Analysis Reports for Pressurized Water Reactors."

DATE
FILMED
10/21/94

END